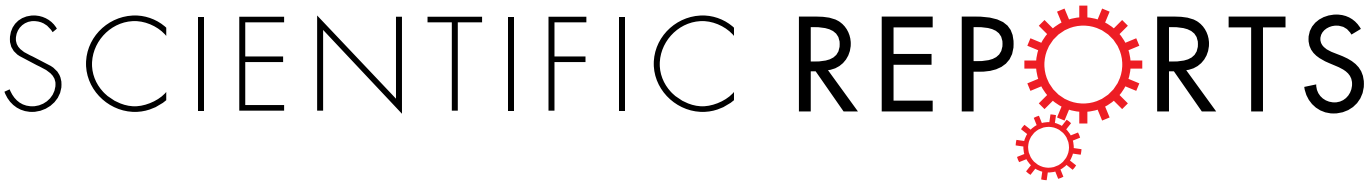

OPEN

Ligustilide, a major bioactive component of *Angelica sinensis*, promotes bone formation via the GPR30/EGFR pathway

Received: 2 January 2019
Accepted: 25 April 2019
Published online: 06 May 2019

F. Yang[1,3], Z. W. Lin[1,3], T. Y. Huang[1,3], T. T. Chen[1,3], J. Cui[1,3], M. Y. Li[1,3] & Y. Q. Hua[1,2,3]

Angelica sinensis* (*Oliv.*) *Diels **is a widely-used traditional Chinese herbal medicine in treating osteoporosis. Ligustilide (LIG) is the main component of *A. sinensis* and is considered to be the most effective biologically active ingredient in this plant. LIG has been found to have multiple pharmacological activities, such as anti-atherosclerosis, neuroprotection, anticancer, anti-inflammatory and analgesic. However, little is known regarding its anti-osteoporotic effects. The aims of this study were to investigate any protective effect of LIG on bone formation. The results showed that LIG significantly ameliorated inhibition of bone formation in zebrafish caused by prednisolone. LIG promoted osteoblast differentiation, including that of the pre-osteoblastic cell line MC3T3-E1 and bone marrow mesenchymal stem cells. LIG greatly improved the viability of MC3T3-E1 cells exposed to H_2O_2, attenuated H_2O_2-induced apoptosis and increased the expression of Bcl-2. Furthermore, LIG treatment lead to marked activation of phosphorylated EGFR and ERK1/2. These effects could be obviously inhibited by blocking GPR30 signaling with the specific inhibitor G15. Collectively, the results reveal that GPR30 is a positive switch for LIG to increase bone formation via regulation of EGFR, and these results provide evidence for the potential of LIG to treat osteoporosis.**

Osteoporosis (OP) is a systemic bone disease characterized by decreased bone mass and degeneration of bone microstructure, resulting in increased fragility of bone, making it prone to fracture[1,2]. Bone mass regulation depends on the dynamic balance between bone formation and bone resorption, which is affected by the activation of osteoblasts or osteoclasts, respectively[3,4]. The main factors affecting bone homeostasis include sex hormones, glucocorticoid administration, cellular inflammatory factors, mechanical forces, and oxidative stress (OS)[5,6]. A decline in estrogen levels has been considered the crucial mechanism of OP. Recent studies indicated that aging and elevated reactive oxygen species (ROS) level are the primary culprits. ROS significantly affect the formation and survival of osteoclasts (OCs), osteoblasts (OBs), and osteocytes[7,8]. Therefore, reducing the OS-induced OB damage is an effective way to prevent or delay the bone loss in OP.

At present, a series of anti-resorptive or anabolic options are commonly used to prevent osteoporotic fractures, especially bisphosphonates, which are the first choice for clinical treatment[9]. However, long-term use of bisphosphonate and denosumab lead to the risk of side effects, such as atypical subtrochanteric fracture or osteonecrosis of the jaw[10]. Therefore, identification of new drugs to treat OP is a worldwide problem and a hot topic. Traditional Chinese medicine (TCM) has unique advantages in the treatment or prevention of OP, and consequently has attracted widespread attention from scholars all around the world[11].

Angelica sinensis (*Oliv.*) *Diels* has a long history of use in traditional herbal medicine. It is traditionally used for treating female disorders including irregular menstruation, amenorrhea and OP[12]. *A. sinensis* is one of the most commonly-used TCMs for the treatment of OP, ranked third and first in the commonly-used TCMs for the treatment of OP and osteoarthritis[13]. Studies confirmed that rats treated with *A. sinensis* showed less trabecular bone loss and thicker cortical areas[14]. The volatile oil is one of the main effective components of *A. sinensis*, and

[1]Jiangsu Key Laboratory for Pharmacology and Safety Evaluation of Chinese Materia Medica, School of Pharmacy, Nanjing University of Chinese Medicine, Nanjing, 210023, China. [2]Jiangsu Collaborative Innovation Center of Chinese Medicinal Resources Industrialization, Nanjing University of Chinese Medicine, Nanjing, 210023, China. [3]School of Pharmacy, Nanjing University of Chinese Medicine, Nanjing, 210023, Jiangsu Province, China. Correspondence and requests for materials should be addressed to Y.Q.H. (email: hua_yq@njucm.edu.cn)

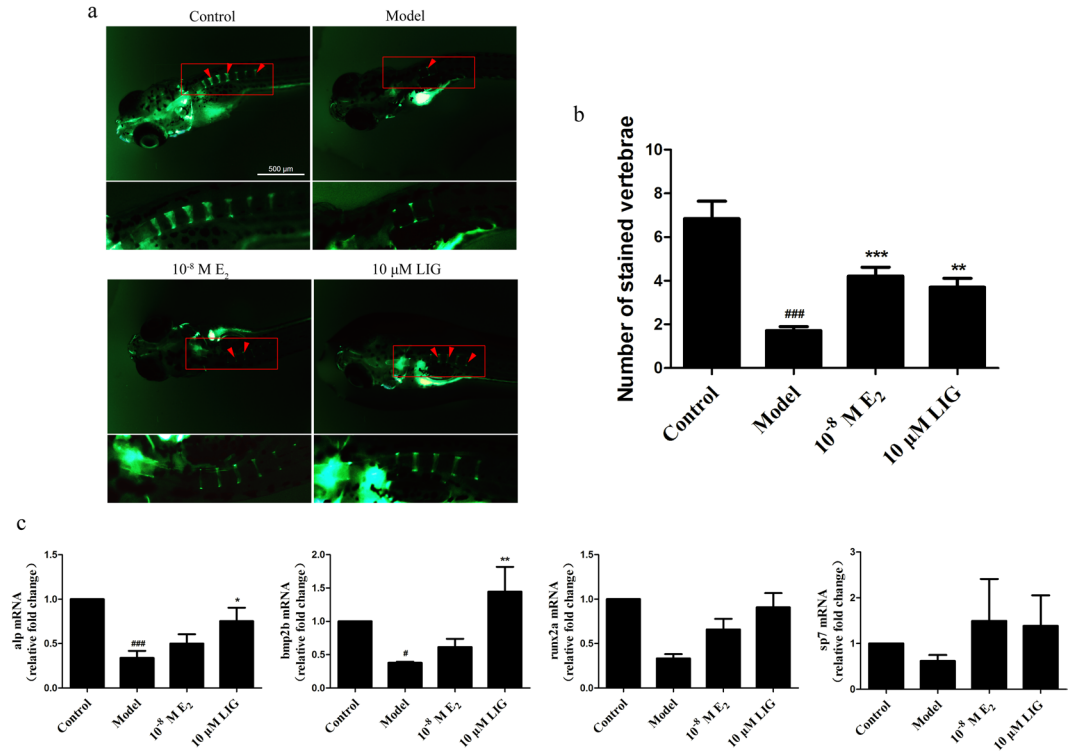

Figure 1. LIG increases bone mass *in vivo*. (**a**) Calcein staining of zebrafish larvae at 9 dpf. Scale bars, 500 μm. Arrowheads, bone calcein staining. (**b**) Number of calcein-stained vertebrae in zebrafish at 9 dpf. Error bars indicate s.e.m., n = 13 for each group. $^{###}P \leq 0.001$ vs. control group. $^{**}P \leq 0.01$, $^{***}P \leq 0.001$ vs. model group. (**c**) The expression mRNA for Alp, Runx2a, sp7, and BMP2b were measured by quantitative RT-PCR in zebrafish at 9 dpf. Error bars indicate s.e.m. (n = 4). $^{#}P \leq 0.05$, $^{###}P \leq 0.001$ vs. control group. $^{*}P \leq 0.05$, $^{**}P \leq 0.01$ vs. model group.

ligustilide (LIG) is the most abundant component in the volatile oil, accounting for approximately 60%[15]. LIG has been found to have multiple pharmacological activities such as anti-atherosclerosis, neuroprotection, anti-cancer, inhibition of cardiac hypertrophy, anti-inflammation and analgesia[16]. Moreover, LIG has been reported to protect skeletal muscle cells, nerve cells, and endothelial cells from all sorts of damage and to have anti-osteoarthritis effects[17–20]. However, it is unclear whether the therapeutic effect of *A. sinensis* on OP is related to LIG. This study found that LIG promotes bone formation by regulating the GPR30/EGFR signaling pathway. Our results provide new insights into the therapeutic mechanism of *A. sinensis* in OP, and provide a basis for its application in the treatment of OP.

Results

LIG improved bone mass in a zebrafish bone-formation-inhibiting model. A bone-formation-inhibiting model was established in zebrafish by treating with prednisolone (Pred; 25 μM)[21]. There is no obvious malformations in embryonic zebrafish treated with prednisolone for 9 days (Supplementary Figure 1a). LIG at 10 μM concentration has no obvious effect on bone mass in normal zebrafish (Supplementary Figure 1b). We then examined the function of LIG in this model, with 17β-estradiol (E_2; 10^{-8} M) used as a positive control[22,23]. Compared with the control group, zebrafish at 3 days post-fertilization (3 dpf) treated with Pred for 6 days showed less bone mass. Compared with the model group, LIG increased the the number of vertebrae and the expression of OB-marker genes (alp, runx2a, sp7 and bmp2b) in zebrafish ($P < 0.05$, $P < 0.01$, $P < 0.001$), showing an equivalent effect to E_2 (Fig. 1).

LIG enhanced the osteogenic differentiation of the pre-osteoblastic cell line MC3T3-E1 and bone marrow mesenchymal stem cells (BMSCs). MC3T3-E1 cells and BMSCs were used to explore the effect of LIG on bone formation *in vitro*. Cells were incubated with OB induction medium (OIM)[24] to induce differentiation. MC3T3-E1 cells displayed a time-dependent development of OB characteristics analogous to *in vivo* bone formation[25]. In these cell cultures, at day 7, no obvious calcified nodules were observed in any group, as assessed by alizarin red staining (Fig. 2a–d). However, by day 14, LIG had significantly enhanced calcified nodule formation compared with the control group (Fig. 2e–h). After 21 days, a large number of calcified nodules had appeared in each group, and there was no obvious difference between the LIG group and the control group (Fig. 2i–l). BMSCs have the ability to differentiate into adipocytes, chondrocytes, and OBs[26,27], and play a key role in regulating bone homeostasis[28]. On the 14th day, in OIM-induced osteogenic differentiated BMSCs, more

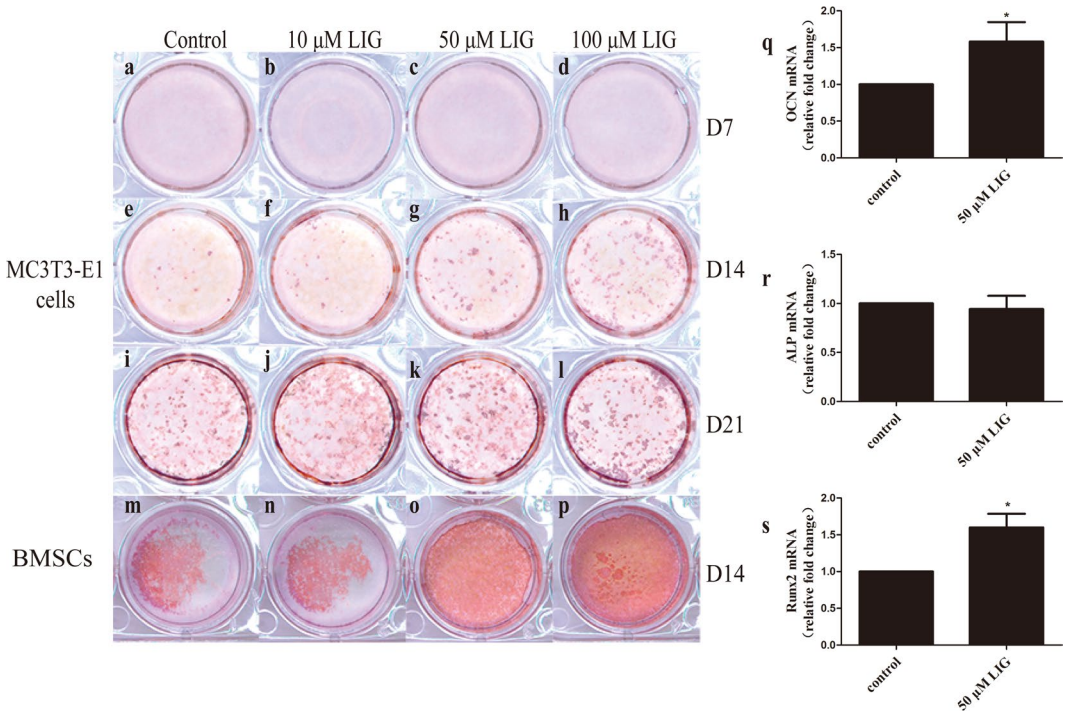

Figure 2. LIG enhances OB differentiation. (**a–l**) Alizarin red staining of MC3T3-E1 cells after 7, 14 and 21 days (D7, 14, 21) in culture under OIM with LIG over the entire culture period. (**m–p**) Alizarin red staining of BMSCs after 14 days (D14) in culture under OIM with LIG over the entire culture period. Pictures taken from a 12-well plate. (**q–s**) The expression mRNA for Alp, Runx2 and OCN were measured by quantitative RT-PCR in BMSCs on the 6th day. Error bars indicate s.e.m. (n = 3). $*P \leq 0.05$ vs. control group.

calcified nodules were observed. Compared with MC3T3-E1 cells, BMSCs possessed greater osteogenic differentiation ability under the same differentiation conditions (Fig. 2 l,m). LIG also promoted osteogenic differentiation of BMSCs (Fig. 2m–p), which was consistent with the effects of LIG *in vivo*. Compared with the control group, 50 μM LIG significantly promoted the expression of OB-marker genes (Runx2 and OCN) in BMSCs on the 6th day. These results demonstrated that the effect of LIG on improving bone mass might be achieved by increasing OB differentiation.

LIG attenuated H_2O_2-induced apoptosis in OBs. A model of peroxidation damage to MC3T3-E1 cells[29] was established to determine the protective effect of LIG on pre-osteoblasts. There was no obvious effect on cell viability after treating with no more than 400 μM H_2O_2 for 4 hours. After that, the cells were cultured for 24 h with complete medium without H_2O_2, and the cell survival rate decreased in a concentration-dependent manner (Fig. 3a,b). Compared with the untreated control group, the cell viability of 200 μM and 400 μM H_2O_2-treated groups significantly decreased approximately 30 to 40%. The cell survival rate of 800 μM and 1,000 μM H_2O_2-treated groups was less than 20%. These results suggested that H_2O_2 damage to cells was a continuous process, and that damage continued to occur even when the level of oxidation in the external environment was reduced.

The level of the anti-apoptotic protein Bcl-2 in H_2O_2-induced OB apoptosis was measured (Fig. 3c–e). Compared with the untreated control group, 200 μM and 400 μM H_2O_2 both significantly decreased the Bcl-2 expression ($P < 0.05$), while no remarkable effect was observed in the expression of the pro-apoptotic protein Bax (Fig. 3d,e).

Although LIG is known to reduce apoptosis in a variety of non-cancerous cells, its effects on oxidative stress-induced OB apoptosis have not been elucidated. LIG at concentrations below 100 μM for 24 h had no effect on MC3T3-E1 cell viability (Fig. 3f). However, when MC3T3-E1 cells were treated with LIG after H_2O_2 exposure and cell viability was measured by MTT assay, the results showed that 50 or 100 μM LIG improved the cell survival rate ($P < 0.01$) (Fig. 3g). Apoptosis was evaluated by flow cytometry, which showed that LIG markedly inhibited apoptosis at concentrations from 1 μM to 100 μM ($P < 0.05$, $P < 0.01$, $P < 0.001$) (Fig. 3h,i).

LIG attenuated H_2O_2-induced apoptosis and promoted differentiation in OBs through GPR30. To understand the mechanism of the anti-apoptotic effect of LIG in MC3T3-E1 cells, the effects of LIG, G15 and ICI182780 on H_2O_2-induced damage were observed by MTT and immunoblotting. When co-treated with 100 nM G15, the GPR30 antagonist, the promotional effect of LIG on cell survival was obviously restrained. This blocking effect was not observed in the 100 nM ICI182780-treated group (Fig. 4a). Previous studies have pointed out that G1, a GPR30 agonist, decreased ROS levels in endothelial cells[30]. GPR30 might thus have a protective effect in

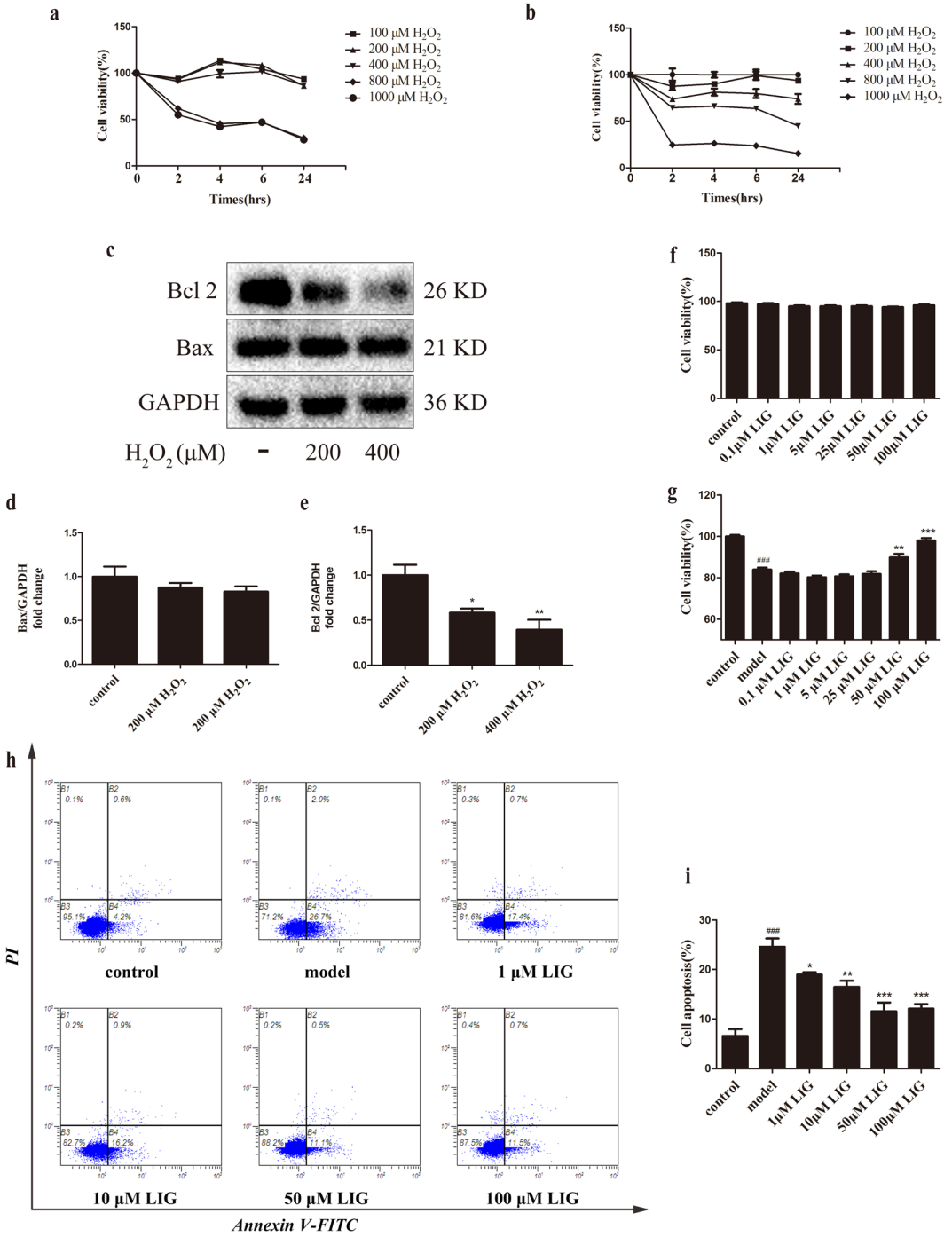

Figure 3. LIG attenuates H_2O_2-induced apoptosis in MC3T3-E1 cells. (**a**,**b**) Cell viability was determined by MTT reduction in MC3T3-E1 cells in the presence of H_2O_2. Error bars indicate s.e.m. (n = 6). (**c**) Representative immunoreactive bands for Bcl-2 and Bax in MC3T3-E1 cells in the presence of H_2O_2. Quantification of immunoreactive bands for Bcl-2 (**d**) and Bax (**e**) relative to GAPDH. Error bars indicate s.e.m. (n = 3). (**f**) and (**g**) Cell viability was determined by MTT reduction in MC3T3-E1 cells with LIG in the presence or absence of H_2O_2. Error bars indicate s.e.m. (n = 18). (**h**) and (**i**) Flow cytometric quantification of apoptosis. Error bars indicate s.e.m. (n = 3). $^{###}P \leq 0.001$ vs. control group. $^{*}P \leq 0.05$, $^{**}P \leq 0.01$, $^{***}P \leq 0.001$ vs. model group.

OBs under oxidative stress. LIG significantly increased the expression of Bcl-2 in MC3T3-E1 cells after peroxidation injury, and this effect was completely abolished by co-treatment with G15 (Fig. 4b).

To explore the mechanism underlying the promotion of osteogenic differentiation by LIG, BMSCs were selected which were more susceptible to differentiation. Compared with the control group, the number of calcified nodules was significantly increased when the BMSCs were treated with 50 μM LIG alone or combined with 100 nM SNG1153 and 100 nM ICI182780. In contrast, compared with the LIG treatment group, the number

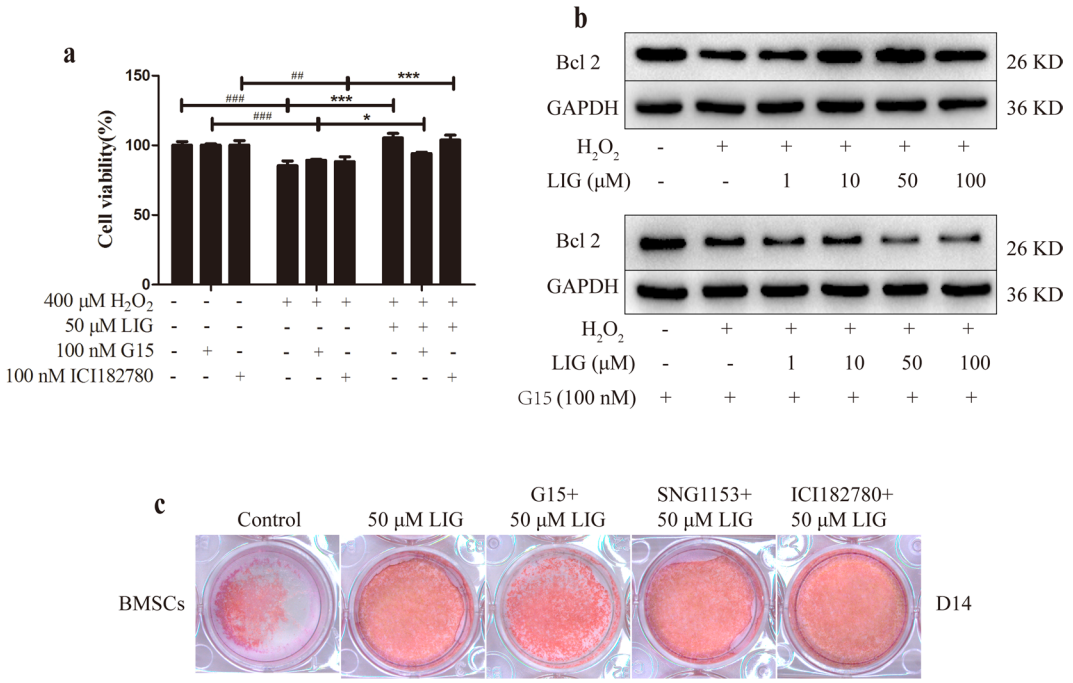

Figure 4. LIG attenuates H_2O_2-induced apoptosis and promotes differentiation in OBs through GPR30. (**a**) Cell viability was measured by MTT reduction in OBs with LIG, G15 and ICI182780 in the presence of H_2O_2. Error bars indicate s.e.m. (n = 6); $^{\#\#}P \leq 0.01$, $^{\#\#\#}P \leq 0.001$ vs. control group. $^{*}P \leq 0.05$, $^{**}P \leq 0.01$, $^{***}P \leq 0.001$ vs. model group. (**b**) Representative immunoblotting images for Bcl-2 in MC3T3-E1 cells with LIG and G15 under oxidative stress. (**c**) Alizarin red staining of BMSCs after 14 days (D14) in culture under OIM with LIG and co-treated with 100 nM G15, 100 nM ICI182780 or 100 nM SNG1153 over the entire culture period.

of calcified nodules was significantly reduced when the BMSCs were treated with LIG combined with 100 nM G15 (Fig. 4c). These results indicated that the promotional effect of LIG on BMSC differentiation was mediated through GPR30.

The anti-apoptotic effect of LIG on OBs was associated with the GPR30/EGFR pathway. As a G protein-coupled estrogen receptor, GPR30 mediates non-genomic rapid responses through activation of the EGFR, MAPK (ERK/p38/JNK), and PI3K/Akt signaling pathways[31,32]. In addition, GPR30 also affects cell proliferation and differentiation by activating EGFR[33]. Within 1 h, LIG (50 μM) significantly promoted activation of the PI3K/Akt and MAPK pathways and phosphorylation of EGFR in MC3T3-E1 cells under oxidative stress (Fig. 5a). It is known that activation of the GPR30/EGFR/ERK pathway promotes cell proliferation and inhibits apoptosis. Treatment with 50 μM LIG and 100 nM G1, the GPR30 agonist, markedly increased the levels of p-EGFR in OBs (Fig. 5b). Co-treatment of 50 μM LIG and 100 nM G15 attenuated activation of the EGFR and ERK1/2 (Fig. 5b,c), while 100 nM G15 and 10 μM AG1478, a specific inhibitor of EGFR[34,35], inhibited accumulation of the anti-apoptotic protein Bcl-2 compared with the 50 μM LIG group (Fig. 5d). These results suggested that LIG might exert anti-apoptotic effects in OBs through the Akt, MAPK and GPR30/EGFR signaling pathways.

Discussion

Our study demonstrated a pharmacological role of LIG in regulation of bone formation and bone mass. Particularly, we found that LIG promotes OB differentiation and prevents pre-osteoblast apoptosis through the GPR30/EGFR pathway.

Estrogen plays a critical role in regulating bone growth through the estrogen receptor[36]. A considerable body of data suggests that the mechanism of estrogen action involves binding to two types of nuclear estrogen receptors (ERα and ERβ)[37]. Recent findings suggested that the novel membrane estrogen receptor GPR30 is involved in non-genomic estrogen signaling[38,39]. GPR30 has been reported to be an essential membrane estrogen receptor for bone development participating in proliferation and differentiation in OBs. G1, a specific agonist of GPR30, promotes bone formation, and G15, a specific antagonist of GPR30, antagonizes the positive effect of G1 on bone[31]. Studies have confirmed that GPR30 is necessary for estradiol or raloxifene-induced proliferation of the human fetal osteoblast hFOB cells[40]. The latest research showed that treatment with 17β-estradiol resulted in the expression of GPR30 and enhanced mitophagy through the GPR30 and ERK1/2 signaling pathways in OBs[41]. In this study, LIG at osteogenic concentrations was unable to activate nuclear ERs including ERα and ERβ, but obviously stimulated GPR30. Among the compounds identified, LIG is thought to be one of the most biologically-active components of *A. sinensis*[42]. This is the first demonstration of selective activation of GPR30 in OBs by a monomeric ingredient of *A. sinensis*.

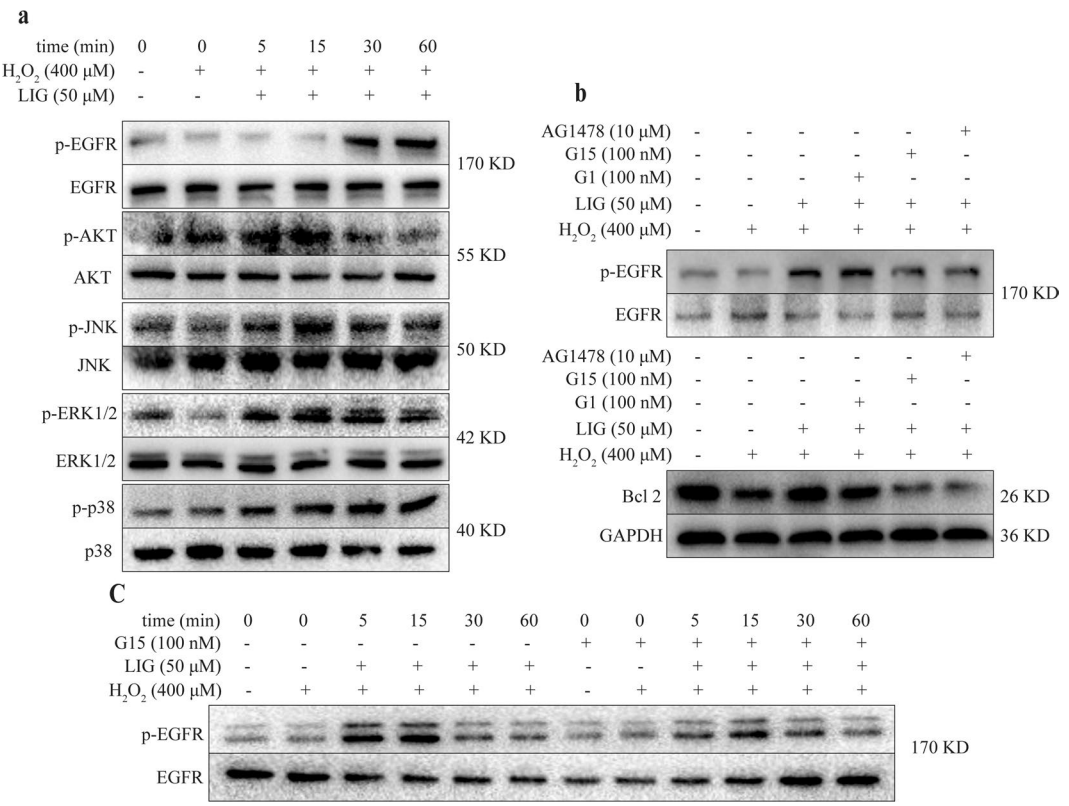

Figure 5. Involvement of GPR30/EGFR/ERK signaling in LIG inhibition of H_2O_2-induced apoptosis in MC3T3-E1 cells. (**a**) Time course of LIG effects on the levels of Akt, p38, JNK, ERK1/2 and EGFR in MC3T3-E1 cells. (**b**) LIG and G1 (100 nM) increased the levels of phosphorylated EGFR (p-EGFR) in MC3T3-E1 cells at 30 min. G15 (100 nM) abolished the effects of LIG and G1 (100 nM). (**c**) LIG increased the levels of phosphorylated ERK1/2 (p-ERK1/2) in MC3T3-E1 cells. G15 abolished the effects of LIG. (**d**) G15 (100 nM) and AG1478 (10 μM) inhibited the level of Bcl-2 induced by LIG in MC3T3-E1 cells.

Signaling mechanisms of GPR30 regulate transcriptional activity involving cAMP, ERK and PI3K[32]. In addition, rapid signaling through GPR30 occurred via transactivation of the epidermal growth factor receptor (EGFR) and involved non-receptor tyrosine kinases of the Src family[33,43]. EGFR activation leads to multiple downstream events, including the activation of PLC, MAPKs, and PI3Ks[33]. This experiment demonstrated that LIG significantly promoted activation of the EGFR, Akt, and MAPK pathways, downstream of GPR30, under oxidative stress in MC3T3-E1 cells. EGFR signaling significantly increased the number of OBs by modulating the proliferation and apoptosis of osteogenic progenitor cells to stimulate bone formation[44]. Studies have found that EGFR controlled bone development by negatively regulating mTOR signaling during the process of OB differentiation[45]. EGF-induced ERK activation in MC3T3-E1 OBs ultimately leads to proliferation and differentiation[46]. Therefore, the mechanism of LIG might be exerted though complex regulation of OBs survival and apoptosis under oxidative stress via the GPR30/EGFR pathway.

A. sinensis is one of the most important TCMs commonly used to invigorate the circulation of blood. With increasing age and associated damage to lipid peroxidation, there would inevitably be microcirculation disturbance and abnormal hemorheology. LIG might be one of the key active ingredients of *A. sinensis* to act on blood circulation. LIG is known to improve cellular antioxidant defense and inhibit H_2O_2-induced apoptosis in PC12 cells[47]. OS-induced OBs apoptosis is crucial to the development of OP[48]. In this study, LIG significantly increased the activity of OBs damaged by H_2O_2 and decreased the apoptosis rate, which might lead to a beneficial effect on bone formation. The antioxidant damage of LIG mentioned above might be related to the blood-activating effect of *A. sinensis*.

The zebrafish model was employed in this study to investigate the bone formation effects of LIG *in vivo*. Because of the molecular and cellular conservation of skeletal development, zebrafish are considered to be an attractive model for *in vivo* screening studies when studying human diseases[49,50]. Low-dose dexamethasone (10 nM) increases ALP content in OBs and promotes OB differentiation[24,51]. In contrast, high-dose glucocorticoids such as prednisolone (25 μM) have been found to have inhibitory effects on bone formation in zebrafish. During ontogenetic growth[52,53], homeostasis, and regeneration of zebrafish bone[21], prednisolone affect the amount, activity and differentiation of OBs, OCs, and immune cells. Here, we showed a therapeutic role of LIG in prednisolone-induced inhibition of bone formation in zebrafish, which was consistent with the effects of LIG *in vitro*.

This study has shown that LIG increases bone mass by promoting OB differentiation and anti-peroxidative damage, and its mechanism might be related to GPR30. The above data indicate that LIG is a beneficial agent in

preventing OP by enhancing bone formation. This suggests that it might be one of the active components of *A. sinensis* functioning in clinical treatment of diseases such as OP and osteoarthritis, and provides more evidence for the clinical application of *A. sinensis* to treat this type of disease. Thus, understanding of the biochemical mechanisms in the GPR30 pathway triggered by LIG might provide some clue for interpreting the action of TCM on bone formation, and might offer more strategies and targets for the treatment of OP.

Methods

Zebrafish studies. Zebrafish (*Danio rerio*) (Ezerinka, NanJing, China) were housed at 28 °C, in a 14 h light and 10 h dark cycle. Zebrafish embryos were collected following natural spawning and raised at 28 °C in E3[24] solution (5 mM NaCl, 0.17 mM KCl, 0.33 mM CaCl, 0.33 mM $MgSO_4$) according to standard protocols. All procedures involving animals were approved by the Animal Care and Use Committee of Nanjing University of Chinese Medicine and strictly performed according to the Guide for the Care and Use of Laboratory Animals.

Prednisolone-induced inhibition of bone formation in zebrafish. Pred (Yuanye, Shanghai, China) was dissolved at 5 mM in 20% dimethyl sulfoxide (DMSO) to create a stock solution. Zebrafish larvae were treated with 25 μM Pred or a corresponding amount of DMSO as control in E3 solution for 6 days, starting at 3 dpf; 10^{-8} M E_2 (Sigma) was used as the positive control. To evaluate bone mass in larvae, live zebrafish were incubated for 1 h in 0.2% calcein (Yuanye) in distilled water (dH_2O) (pH 7), then rinsed in water three times, and incubated in dH_2O for 1 h. The zebrafish were anesthetized with 0.02% Tricaine (MS222) and imaged under a fluorescence microscope (Leica, M205 FA, Leica Microsystems Ltd., Wetzlar Germany). Measurements of intracranial bone area were carried out using the Plot Profile tool in Image J[21].

Cell culture. The pre-osteoblasts (MC3T3-E1 cells) used in this study were obtained from the cell library of Shanghai Chinese Academy of Sciences (Shanghai, China). Bone marrow mesenchymal stem cells (BMSCs) were isolated from the femurs of neonatal rats (1 to 2 weeks old) following the method described by Huang[54], with slight modifications. BMSCs were cultured in α-MEM (Gibco, Grand Island, NY, USA). MC3T3-E1 cells and BMSCs were maintained in α-MEM supplemented with 10% fetal bovine serum (FBS; Gibco) and 1% penicillin–streptomycin (P/S; TransGen Biotech, Beijing, China) in a humidified incubator at 37 °C with 5% CO_2.

OB differentiation. For OB differentiation, MC3T3-E1 cells and BMSCs were seeded into 12-well plates (1×10^5 cells/well) and induced with OB induction medium (OIM)[24] consisting of α-MEM containing 10 mM β-glycerophosphate (Sigma, St. Louis, MO, USA), 10 nM dexamethasone (Dex; Sigma), and 50 mg/mL L-ascorbic acid (Sigma) supplemented with 10% FBS and 1% P/S. Mineralized matrix formation by OB was observed by alizarin red staining (Servicebio, Wuhan, China) examined under a stereomicroscope (ZEISS, Stemi 2000-C; Carl Zeiss Microscopy GmbH, Jena, Germany).

Cell treatments. The final concentrations of the compounds were as follows: H_2O_2 (100, 200, 400, 800, 1,000 and 2,000 μM; Ningshi, Nanjing, China), the GPR30 antagonist G15 (100 nM; Caymanchem, Wuhan, China), the GPR30 agonist G1 (100 nM; Caymanchem), the ER-α 36 antagonist SNG1153 (100 nM; MCE, Princeton, NJ, USA), the ER antagonist ICI182780 (100 nM; Tocris, Massachusetts, USA), EGFR inhibitor AG1478 (10 μM; Selleckchem, Shanghai, China), and LIG (1, 10, 50, and 100 μM; ZZBio Co. Ltd., Shanghai, China). The final concentration of the vehicle, DMSO, was less than 0.5% in all experiments. MC3T3-E1 cells were treated with or without H_2O_2 and the indicated test compounds for various times, according to the experimental protocol.

Cell viability assay. MC3T3-E1 cells were seeded into 96-well plates (1×10^4 cells/well) and cultured under various conditions, as indicated for each experiment. Serum-free α-MEM (200 μL) supplemented with 20 μL MTT solution (5 mg/mL; NeoFroxx, Einhausen, Germany) was added to each well, and cells were further incubated at 37 °C. After 4 h, the MTT medium was removed, and the formazan crystals were dissolved in 150 μL DMSO. The absorbance of the plates was then measured in a microplate reader (BioTek, SyneRgy2; BioTek, Winooski, VT, USA) at 490 nm.

Flow cytometry. After treatments, MC3T3-E1 cells were analyzed by Annexin V-FITC/PI double staining, and then cytofluorometric analysis was performed by Flow Cytometry (Beckman Coulter, Brea, CA, USA).

Western blot analyses. After treatments, MC3T3-E1 cells were lysed in cell lysis buffer (Applygen, Beijing, China). Protein concentration was assayed using the BCA protein Assay kit (Beyotime, Shanghai, China). Aliquots containing 20 μg cell protein were separated on 10% SDS-PAGE gels and transferred to polyvinylidene difluoride membranes (Millipore, Darmstadt, Germany) using the Trans-Blot Turbo system (BioRad, Hercules, CA, USA). Anti-phospho-Akt Ser473 (1:1,000; Proteintech, Chicago, IL, USA), anti-Akt (1:1,000; Proteintech), anti-phospho-EGFR (1:1,000; Cell Signaling Technology, Danvers, MA, USA), anti-EGFR (1:1,000; Abcam, Cambridge, UK), anti-phospho-JNK (1:1,000; Abcam), anti-JNK (1:1,000; Cell Signaling Technology), anti-phospho-ERK1/2 (1:1,000; Affbiotech, Changzhou, China), anti-ERK1/2 (1:1,000; Proteintech), anti-phospho-p38 (1:1,000; Abcam), anti-p38 (1:1,000; Abcam), anti-Bcl-2 (1:1,000; Abcam), anti-Bax (1:1,000; Proteintech) and anti-GAPDH antibodies were used as primary antibodies, followed by addition of an appropriate secondary antibody (1:10,000). After antibody incubation, an enhanced chemiluminescence substrate (Millipore) was added and the protein bands were detected using a Bio-Rad ChemiDoc XRS^+ Image station (BioRad). The images were quantitated using Image Lab software.

RT-qPCR. Total RNA was isolated and purified by RNA isolater® Total RNA Extraction Reagent (Vazyme Biotech, Nanjing, China). RNA concentrations were determined using Synergy2 Multi-mode Microplate Reader.

cDNA was synthesized from 1 mg total RNA using HiScript® II Q RT SuperMix for qPCR (+g DNA wiper) (Vazyme Biotech, Nanjing, China). Real-time PCR was then conducted with the ABI 7500 Sequencing Detection System (Applied Biosystems, Foster City, CA, United States) and the AceQ® qPCR SYBR® Green Master Mix (Vazyme Biotech, Q111-02). Samples were analyzed using a 7500 fast real time PCR System (Applied Biosystems, Foster City, CA, USA). Two microlitres of each cDNA were subjected to PCR amplification using specific primers as follows: bmp2b (F) 5′-CGGTCAACTCCAACATTCCC-3′, (R) 5′-ATTGTTCTCATCGGCAACCG-3′; sp7 (F) 5′-TGGATTGACCCTCACTGGAC-3′, (R) 5′-GATGGTGCTTCCCGGTTTAC-3′; runx2a (F) 5′-GTGGAGATCATAGCGGACCA-3′, (R) 5′-CTCCCAGAGCCACAACCTTA-3′; alp (F) 5′-GGCCTTACATGAAGCTGTGG-3′, (R) 5′-GTTTCCTCGTGGTGTGTAGC-3′; gapdh (F) 5′-TGGTGCTGGTATTGCTCTCA-3′, (R) 5′-ATGGGAGAATGGTCGCGTAT-3′; Runx2 (F) 5′-CATCCTTCCCTCCGAGACCCTAA-3′, (R) 5′-CCCAACATGGCTGCTCCCTTC-3′; OCN (F) 5′-CTCACTCTGCTGGCCCTGAC-3′, (R) 5′-CACCTTACTGCCCTCCTGCTTG-3′; Alp (F) 5′-AGGGTGGGTTTCTCTCTTGG-3′, (R) 5′-CATGATGGTTGCAGGGTCTG-3′; GAPDH (F) 5′-TGAACGGGAAGCTCACTGG-3′, (R) 5′-TCCACCACCCTGTTGCTGTA-3′.

Data analysis. All data are displayed as means ± standard error (s.e.m.). All statistical analyses were performed on GraphPad Prism 5.0 (GraphPad Software, San Diego, CA, USA). Statistical analysis with multiple comparisons was performed with one-way ANOVA, and differences between treatment groups were considered significant if $P < 0.05$.

Data Availability

All data discussed in this report are available upon request.

References

1. Shan, P. F., Xian, C. J., Li, M., Xiang, G. D. & Yuan, L. Q. Osteoporosis. *Int J Endocrinol* **2013**, 952858, https://doi.org/10.1155/2013/952858 (2013).
2. Tu, K. N. *et al*. Osteoporosis: A Review of Treatment Options. *P T* **43**, 92–104 (2018).
3. Luo, J. *et al*. LGR4 is a receptor for RANKL and negatively regulates osteoclast differentiation and bone resorption. *Nat Med* **22**, 539–546, https://doi.org/10.1038/nm.4076 (2016).
4. Manolagas, S. C. & Jilka, R. L. Bone marrow, cytokines, and bone remodeling. *Emerging insights into the pathophysiology of osteoporosis. N Engl J Med* **332**, 305–311, https://doi.org/10.1056/NEJM199502023320506 (1995).
5. Hendrickx, G., Boudin, E. & Van Hul, W. A look behind the scenes: the risk and pathogenesis of primary osteoporosis. *Nat Rev Rheumatol* **11**, 462–474, https://doi.org/10.1038/nrrheum.2015.48 (2015).
6. Panontin, E., Rizzello, E. & Ventura, A. Vertebral fractures. *N Engl J Med* **365**, 673, author reply 674, https://doi.org/10.1056/NEJMc1106933 (2011).
7. Manolagas, S. C. From estrogen-centric to aging and oxidative stress: a revised perspective of the pathogenesis of osteoporosis. *Endocr Rev* **31**, 266–300, https://doi.org/10.1210/er.2009-0024 (2010).
8. Wilson, C. B. Oxidative stress and osteoporosis. *Nat Rev Endocrinol* **10**, 3, https://doi.org/10.1038/nrendo.2013.225 (2014).
9. Das, S. & Crockett, J. C. Osteoporosis - a current view of pharmacological prevention and treatment. *Drug Des Devel Ther* **7**, 435–448, https://doi.org/10.2147/DDDT.S31504 (2013).
10. Crandall, C. J. *et al*. Comparative effectiveness of pharmacologic treatments to prevent fractures: an updated systematic review. *Ann Intern Med* **161**, 711–723, https://doi.org/10.7326/M14-0317 (2014).
11. Zhao, H. *et al*. Prevention and Treatment of Osteoporosis Using Chinese Medicinal Plants: Special Emphasis on Mechanisms of Immune Modulation. *J Immunol Res* **2018**, 6345857, https://doi.org/10.1155/2018/6345857 (2018).
12. Wei, W. L., Zeng, R., Gu, C. M., Qu, Y. & Huang, L. F. Angelica sinensis in China-A review of botanical profile, ethnopharmacology, phytochemistry and chemical analysis. *J Ethnopharmacol* **190**, 116–141, https://doi.org/10.1016/j.jep.2016.05.023 (2016).
13. Zheng, Z. R. & Tang, S. H. Comparative analysis on composition principles of traditional Chinese medicine prescriptions for osteoporosis and osteoarthritis. *Zhongguo Zhong Yao Za Zhi* **39**, 3172–3175 (2014).
14. Choi, K. O. *et al*. Ultrafine Angelica gigas powder normalizes ovarian hormone levels and has antiosteoporosis properties in ovariectomized rats: particle size effect. *J Med Food* **15**, 863–872, https://doi.org/10.1089/jmf.2011.2047 (2012).
15. Zeng, Q. *et al*. Quick and selective extraction of Z-ligustilide from Angelica sinensis using magnetic multiwalled carbon nanotubes. *J Sep Sci* **38**, 4269–4275, https://doi.org/10.1002/jssc.201500862 (2015).
16. Zuo, A. H., Wang, L. & Xiao, H. B. Research progress studies on pharmacology and pharmacokinetics of ligustilide. *Zhongguo Zhong Yao Za Zhi* **37**, 3350–3353 (2012).
17. Li, X. *et al*. The Protective Effect of Ligustilide in Osteoarthritis: An *in Vitro* and *in Vivo* Study. *Cell Physiol Biochem* **48**, 2583–2595, https://doi.org/10.1159/000492701 (2018).
18. Shi, Y. *et al*. Ligustilide prevents the apoptosis effects of tumour necrosis factor-alpha during C2C12 cell differentiation. *Int Immunopharmacol* **19**, 358–364, https://doi.org/10.1016/j.intimp.2014.02.007 (2014).
19. Long, F. Y. *et al*. Klotho upregulation contributes to the neuroprotection of ligustilide against cerebral ischemic injury in mice. *Eur J Pharmacol* **820**, 198–205, https://doi.org/10.1016/j.ejphar.2017.12.019 (2018).
20. Choi, E. S. *et al*. Ligustilide attenuates vascular inflammation and activates Nrf2/HO-1 induction and, NO synthesis in HUVECs. *Phytomedicine* **38**, 12–23, https://doi.org/10.1016/j.phymed.2017.09.022 (2018).
21. Geurtzen, K. *et al*. Immune Suppressive and Bone Inhibitory Effects of Prednisolone in Growing and Regenerating Zebrafish Tissues. *J Bone Miner Res* **32**, 2476–2488, https://doi.org/10.1002/jbmr.3231 (2017).
22. Chaturantabut, S. *et al*. Estrogen Activation of G protein-coupled Estrogen Receptor 1 Regulates Phosphoinositide 3-kinase and mTOR Signaling to Promote Liver Growth in Zebrafish and Proliferation of Human Hepatocytes. *Gastroenterology*, https://doi.org/10.1053/j.gastro.2019.01.010 (2019).
23. Barrett, R., Chappell, C., Quick, M. & Fleming, A. A rapid, high content, *in vivo* model of glucocorticoid-induced osteoporosis. *Biotechnol J* **1**, 651–655, https://doi.org/10.1002/biot.200600043 (2006).
24. Jafari, A. *et al*. Legumain Regulates Differentiation Fate of Human Bone Marrow Stromal Cells and Is Altered in Postmenopausal Osteoporosis. *Stem Cell Reports* **8**, 373–386, https://doi.org/10.1016/j.stemcr.2017.01.003 (2017).
25. Quarles, L. D., Yohay, D. A., Lever, L. W., Caton, R. & Wenstrup, R. J. Distinct proliferative and differentiated stages of murine MC3T3-E1 cells in culture: an *in vitro* model of osteoblast development. *J Bone Miner Res* **7**, 683–692, https://doi.org/10.1002/jbmr.5650070613 (1992).
26. Bianco, P. *et al*. The meaning, the sense and the significance: translating the science of mesenchymal stem cells into medicine. *Nat Med* **19**, 35–42, https://doi.org/10.1038/nm.3028 (2013).
27. Shen, G. *et al*. GOLM1 Stimulation of Glutamine Metabolism Promotes Osteoporosis via Inhibiting Osteogenic Differentiation of BMSCs. *Cell Physiol Biochem* **50**, 1916–1928, https://doi.org/10.1159/000494872 (2018).

28. Liu, Y. *et al*. Hydrogen sulfide maintains mesenchymal stem cell function and bone homeostasis via regulation of Ca(2+) channel sulfhydration. *Cell Stem Cell* **15**, 66–78, https://doi.org/10.1016/j.stem.2014.03.005 (2014).
29. Fu, C. *et al*. Alpha-Lipoic Acid Promotes Osteoblastic Formation in H_2O_2 -Treated MC3T3-E1 Cells and Prevents Bone Loss in Ovariectomized Rats. *J Cell Physiol* **230**, 2184–2201, https://doi.org/10.1002/jcp.24947 (2015).
30. Kong, B. S., Cho, Y. H. & Lee, E. J. G protein-coupled estrogen receptor-1 is involved in the protective effect of protocatechuic aldehyde against endothelial dysfunction. *PLoS One* **9**, e113242, https://doi.org/10.1371/journal.pone.0113242 (2014).
31. Kang, W. B. *et al*. Osteoprotective effects of estrogen membrane receptor GPR30 in ovariectomized rats. *J Steroid Biochem Mol Biol* **154**, 237–244, https://doi.org/10.1016/j.jsbmb.2015.07.002 (2015).
32. Prossnitz, E. R. *et al*. Estrogen signaling through the transmembrane G protein-coupled receptor GPR30. *Annu Rev Physiol* **70**, 165–190, https://doi.org/10.1146/annurev.physiol.70.113006.100518 (2008).
33. Filardo, E. J., Quinn, J. A., Bland, K. I. & Frackelton, A. R. Jr. Estrogen-induced activation of Erk-1 and Erk-2 requires the G protein-coupled receptor homolog, GPR30, and occurs via trans-activation of the epidermal growth factor receptor through release of HB-EGF. *Mol Endocrinol* **14**, 1649–1660, https://doi.org/10.1210/mend.14.10.0532 (2000).
34. Weller, M. L. *et al*. Epidermal growth factor receptor is a co-receptor for adeno-associated virus serotype 6. *Nat Med* **16**, 662–664, https://doi.org/10.1038/nm.2145 (2010).
35. Zeboudj, L. *et al*. Selective EGF-Receptor Inhibition in CD4(+) T Cells Induces Anergy and Limits Atherosclerosis. *J Am Coll Cardiol* **71**, 160–172, https://doi.org/10.1016/j.jacc.2017.10.084 (2018).
36. Brann, D. W., Dhandapani, K., Wakade, C., Mahesh, V. B. & Khan, M. M. Neurotrophic and neuroprotective actions of estrogen: basic mechanisms and clinical implications. *Steroids* **72**, 381–405, https://doi.org/10.1016/j.steroids.2007.02.003 (2007).
37. Deroo, B. J. & Korach, K. S. Estrogen receptors and human disease. *J Clin Invest* **116**, 561–570, https://doi.org/10.1172/JCI27987 (2006).
38. Windahl, S. H. *et al*. The role of the G protein-coupled receptor GPR30 in the effects of estrogen in ovariectomized mice. *Am J Physiol Endocrinol Metab* **296**, E490–496, https://doi.org/10.1152/ajpendo.90691.2008 (2009).
39. Khan, K. *et al*. Prunetin signals via G-protein-coupled receptor, GPR30(GPER1): Stimulation of adenylyl cyclase and cAMP-mediated activation of MAPK signaling induces Runx2 expression in osteoblasts to promote bone regeneration. *J Nutr Biochem* **26**, 1491–1501, https://doi.org/10.1016/j.jnutbio.2015.07.021 (2015).
40. Noda-Seino, H. *et al*. Estradiol and raloxifene induce the proliferation of osteoblasts through G-protein-coupled receptor GPR30. *J Endocrinol Invest* **36**, 21–27, https://doi.org/10.3275/8301 (2013).
41. Sun, X., Yang, X., Zhao, Y., Li, Y. & Guo, L. Effects of 17β-Estradiol on Mitophagy in the Murine MC3T3-E1 Osteoblast Cell Line is Mediated via G Protein-Coupled Estrogen Receptor and the ERK1/2 Signaling Pathway. *Medical Science Monitor* **24**, 903–911, https://doi.org/10.12659/msm.908705 (2018).
42. Zhang, X. G. *et al*. A novel enzyme-assisted approach for efficient extraction of Z-ligustilide from Angelica sinensis plants. *Sci Rep* **7**, 9783, https://doi.org/10.1038/s41598-017-10004-x (2017).
43. Prenzel, N. *et al*. EGF receptor transactivation by G-protein-coupled receptors requires metalloproteinase cleavage of proHB-EGF. *Nature* **402**, 884–888, https://doi.org/10.1038/47260 (1999).
44. Chandra, A., Lan, S., Zhu, J., Siclari, V. A. & Qin, L. Epidermal growth factor receptor (EGFR) signaling promotes proliferation and survival in osteoprogenitors by increasing early growth response 2 (EGR2) expression. *J Biol Chem* **288**, 20488–20498, https://doi.org/10.1074/jbc.M112.447250 (2013).
45. Linder, M. *et al*. EGFR controls bone development by negatively regulating mTOR-signaling during osteoblast differentiation. *Cell Death Differ* **25**, 1094–1106, https://doi.org/10.1038/s41418-017-0054-7 (2018).
46. Saito, K. *et al*. Conditional inactivation of TNFalpha-converting enzyme in chondrocytes results in an elongated growth plate and shorter long bones. *PLoS One* **8**, e54853, https://doi.org/10.1371/journal.pone.0054853 (2013).
47. Yu, Y., Du, J. R., Wang, C. Y. & Qian, Z. M. Protection against hydrogen peroxide-induced injury by Z-ligustilide in PC12 cells. *Exp Brain Res* **184**, 307–312, https://doi.org/10.1007/s00221-007-1100-3 (2008).
48. Moriishi, T. *et al*. Bcl2 deficiency activates FoxO through Akt inactivation and accelerates osteoblast differentiation. *PLoS One* **9**, e86629, https://doi.org/10.1371/journal.pone.0086629 (2014).
49. Grimes, D. T. *et al*. Zebrafish models of idiopathic scoliosis link cerebrospinal fluid flow defects to spine curvature. *Science* **352**, 1341–1344, https://doi.org/10.1126/science.aaf6419 (2016).
50. Hayes, M. *et al*. ptk7 mutant zebrafish models of congenital and idiopathic scoliosis implicate dysregulated Wnt signalling in disease. *Nat Commun* **5**, 4777, https://doi.org/10.1038/ncomms5777 (2014).
51. Oshina, H. *et al*. Effects of continuous dexamethasone treatment on differentiation capabilities of bone marrow-derived mesenchymal cells. *Bone* **41**, 575–583, https://doi.org/10.1016/j.bone.2007.06.022 (2007).
52. Canalis, E. Mechanisms of glucocorticoid-induced osteoporosis. *Curr Opin Rheumatol* **15**, 454–457 (2003).
53. Canalis, E. & Delany, A. M. Mechanisms of glucocorticoid action in bone. *Ann N Y Acad Sci* **966**, 73–81 (2002).
54. Huang, J., Zhao, L., Xing, L. & Chen, D. MicroRNA-204 regulates Runx2 protein expression and mesenchymal progenitor cell differentiation. *Stem Cells* **28**, 357–364, https://doi.org/10.1002/stem.288 (2010).

Acknowledgements

We thank Dr. L. Yu for zebrafish experimental technical support. This research was supported by grants from the National Natural Science Foundation of China (81473390, 30902014), the Jiangsu Collaborative Innovation Center of Chinese Medicinal Resources Industrialization (No. 012092002001-7), the Open Project Program of Jiangsu Key Laboratory for Pharmacology and Safety Evaluation of Chinese Materia Medica (No. JKLPSE201818) and the Project of the Priority Academic Program Development of Jiangsu Higher Education Institutions (PAPD).

Author Contributions

H.Y.Q., Y.F. and L.Z.W. designed the experiment. Y.F. contributed to all experiments and the manuscript preparation. L.Z.W. performed the osteoblast differentiation study. H.T.Y. performed the *in vivo* study. C.T.T. performed the western blot experiments. All authors contributed to drafting the manuscript and designing the figures.

Additional Information

Supplementary information accompanies this paper at https://doi.org/10.1038/s41598-019-43518-7.

Competing Interests: The authors declare no competing interests.

Publisher's note: Springer Nature remains neutral with regard to jurisdictional claims in published maps and institutional affiliations.